

ABCA4 Gene Screening by Next-Generation Sequencing in a British Cohort

Kaoru Fujinami,¹⁻⁴ Jana Zernant,⁵ Ravinder K. Chana,^{3,4} Genevieve A. Wright,^{3,4} Kazushige Tsunoda,¹ Yoko Ozawa,² Kazuo Tsubota,² Andrew R. Webster,^{3,4} Anthony T. Moore,^{3,4} Rando Allikmets,^{5,6} and Michel Michaelides^{3,4}

¹Laboratory of Visual Physiology, National Institute of Sensory Organs, National Tokyo Medical Center, Tokyo, Japan

²Department of Ophthalmology, Keio University, School of Medicine, Tokyo, Japan

³UCL Institute of Ophthalmology, London, United Kingdom

⁴Moorfields Eye Hospital, London, United Kingdom

⁵Department of Ophthalmology, Columbia University, New York, New York

⁶Department of Pathology and Cell Biology, Columbia University, New York, New York

Correspondence: Rando Allikmets, Columbia University, 630 West 168th Street, New York, NY 10032; rla22@columbia.edu.

Michel Michaelides, UCL Institute of Ophthalmology, 11-43 Bath Street, London, EC1V 9EL, UK; michel.michaelides@ucl.ac.uk.

Submitted: June 9, 2013

Accepted: August 19, 2013

Citation: Fujinami K, Zernant J, Chana RK, et al. *ABCA4* gene screening by next-generation sequencing in a British cohort. *Invest Ophthalmol Vis Sci.* 2013;54:6662-6674. DOI:10.1167/iov.13-12570

PURPOSE. We applied a recently reported next-generation sequencing (NGS) strategy for screening the *ABCA4* gene in a British cohort with *ABCA4*-associated disease and report novel mutations.

METHODS. We identified 79 patients with a clinical diagnosis of *ABCA4*-associated disease who had a single variant identified by the *ABCA4* microarray. Comprehensive phenotypic data were obtained, and the NGS strategy was applied to identify the second allele by means of sequencing the entire coding region and adjacent intronic sequences of the *ABCA4* gene. Identified variants were confirmed by Sanger sequencing and assessed for pathogenicity by in silico analysis.

RESULTS. Of the 42 variants detected by prescreening with the microarray, in silico analysis suggested that 34, found in 66 subjects, were disease-causing and 8, found in 13 subjects, were benign variants. We detected 42 variants by NGS, of which 39 were classified as disease-causing. Of these 39 variants, 31 were novel, including 16 missense, 7 splice-site-altering, 4 nonsense, 1 in-frame deletion, and 3 frameshift variants. Two or more disease-causing variants were confirmed in 37 (47%) of 79 patients, one disease-causing variant in 36 (46%) subjects, and no disease-causing variant in 6 (7%) individuals.

CONCLUSIONS. Application of the NGS platform for *ABCA4* screening enabled detection of the second disease-associated allele in approximately half of the patients in a British cohort where one mutation had been detected with the arrayed primer extension (APEX) array. The time- and cost-efficient NGS strategy is useful in screening large cohorts, which will be increasingly valuable with the advent of *ABCA4*-directed therapies.

Keywords: *ABCA4*, next generation sequencing, Stargardt disease

Stargardt disease is the most common form of inherited macular dystrophy and is caused by recessive mutations in the *ABCA4* gene.^{1,2} Stargardt disease typically presents with central macular atrophy and yellow-white flecks at the posterior pole, primarily at the level of the RPE.^{2,3} A highly variable phenotype and progression of Stargardt disease have been documented, and mutations in *ABCA4* also have been implicated in cone dystrophy, cone-rod dystrophy, and "retinitis pigmentosa."⁴⁻¹² In this report, we will use the term "*ABCA4*-associated retinal disease" to refer to the broad range and variability of clinical manifestations of retinopathy due to *ABCA4* variants.

The carrier frequency of likely pathogenic *ABCA4* alleles has been reported to be as high as 1:20^{13,14} and more than 700 *ABCA4* variants have been identified so far.^{1,2,5-29} The high allelic heterogeneity makes molecular genetic analyses of *ABCA4*-associated retinal disease very challenging. It has been reported that direct Sanger sequencing of the entire *ABCA4* coding region (50 exons) detects between 66% and 80% of

disease-causing alleles^{13,21}; however, this approach has significant limitations in large patient cohorts due to the prohibitive time and cost implications.^{3,5}

Since the development of the *ABCA4* genotyping microarray, using arrayed primer extension (APEX) technology,¹⁴ systematic screening of all known previously reported *ABCA4* variants has been available^{26,30}; APEX detects approximately 65% to 75% of all disease-associated alleles. However, by definition, novel variants are not detected by APEX technology, necessitating the use of other methodologies for high-throughput systematic screening of the entire coding region, especially in cases where one or both disease-causing alleles have failed to be identified by the array.

Zernant et al. recently reported the capability of a next-generation sequencing (NGS) strategy to detect new *ABCA4* variants that were not included on the APEX array; all 50 *ABCA4* exons of 168 patients were amplified in parallel using an amplicon tagging PCR protocol and NGS was applied to the resulting amplicons.⁵ The purpose of this study was to apply this

TABLE 1. Summary of Clinical Features of 79 Patients With *ABCA4*-Related Retinal Disease

Median age of onset, y (range)		22.0 (5-71)
Median age at examination, y (range)		40.0 (15-79)
Median duration of disease, y (range)		10.0 (0-54)
LogMAR visual acuity (range)	R	1.00 (-0.08-1.78)
	L	1.00 (-0.08-4.00)
AF subtype, <i>n</i> = 71	1	<i>n</i> = 21
	2	<i>n</i> = 34
	3	<i>n</i> = 16
ERG group, <i>n</i> = 70	1	<i>n</i> = 34
	2	<i>n</i> = 7
	3	<i>n</i> = 29

AF, autofluorescence; ERG, electroretinography; R, right eye; L, left eye.

novel NGS strategy for *ABCA4* screening in a large, well-characterized British cohort of patients with likely *ABCA4*-associated phenotypes and report novel disease-causing variants.

MATERIALS AND METHODS

Patients

Prescreening with APEX technology was performed in a cohort of 232 patients seen at Moorfields Eye Hospital with a clinical diagnosis of retinopathy compatible with *ABCA4*-associated retinal disease. Two or more variants were identified in 103 patients, one variant in 79 subjects, and no variants in 50 individuals. The 79 patients with only one *ABCA4* allele were recruited for this study. After informed consent was obtained, blood samples were taken from all individuals for NGS of *ABCA4*. The protocol of the study adhered to the provisions of the Declaration of Helsinki and was approved by the Ethics Committee of Moorfields Eye Hospital. The age at onset was defined as the age at which visual loss was first noted by the patient. The duration of

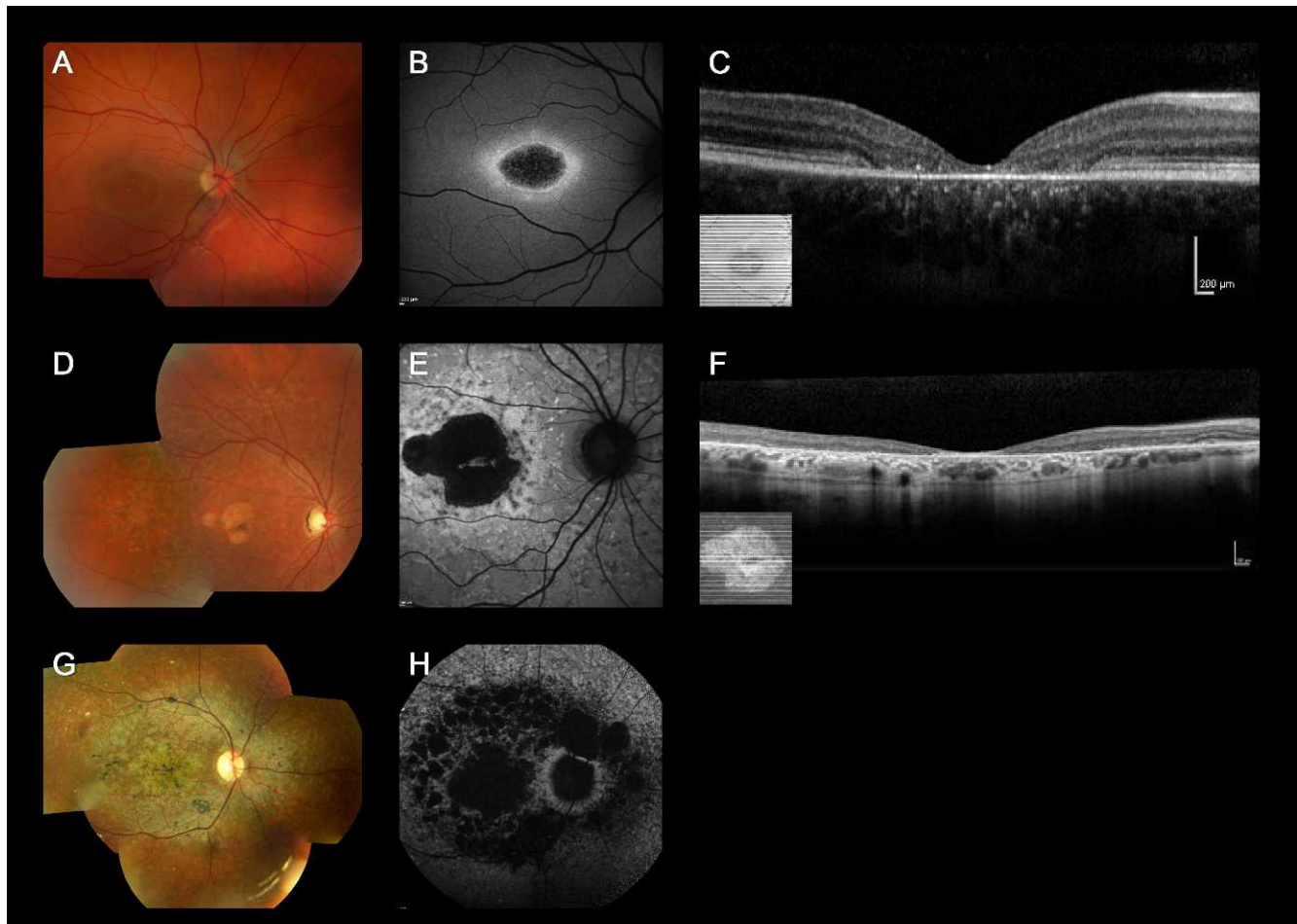


FIGURE 1. Color fundus photographs, autofluorescence images, and optical coherence tomography of three representative cases harboring two or more *ABCA4* variants with “typical” *ABCA4*-associated retinal disease (patients 19, 36, and 17). Color fundus photograph of patient 19 shows macular atrophy (A) and AF imaging demonstrates a localized low AF signal at the fovea, with a high signal edge surrounded by a homogeneous background (B). SD-OCT demonstrates marked outer retinal loss at the central macula (C). Patient 36 has macular atrophy surrounded by numerous yellow-white flecks (D) and a localized low AF signal at the macula surrounded by a heterogeneous background, with peripapillary sparing (E). Generalized loss of outer retinal architecture is seen on SD-OCT. Patient 17 has widespread multiple areas of atrophy with patchy pigmentation (G) and multiple areas of low AF signal at the posterior pole with a heterogeneous background (H).

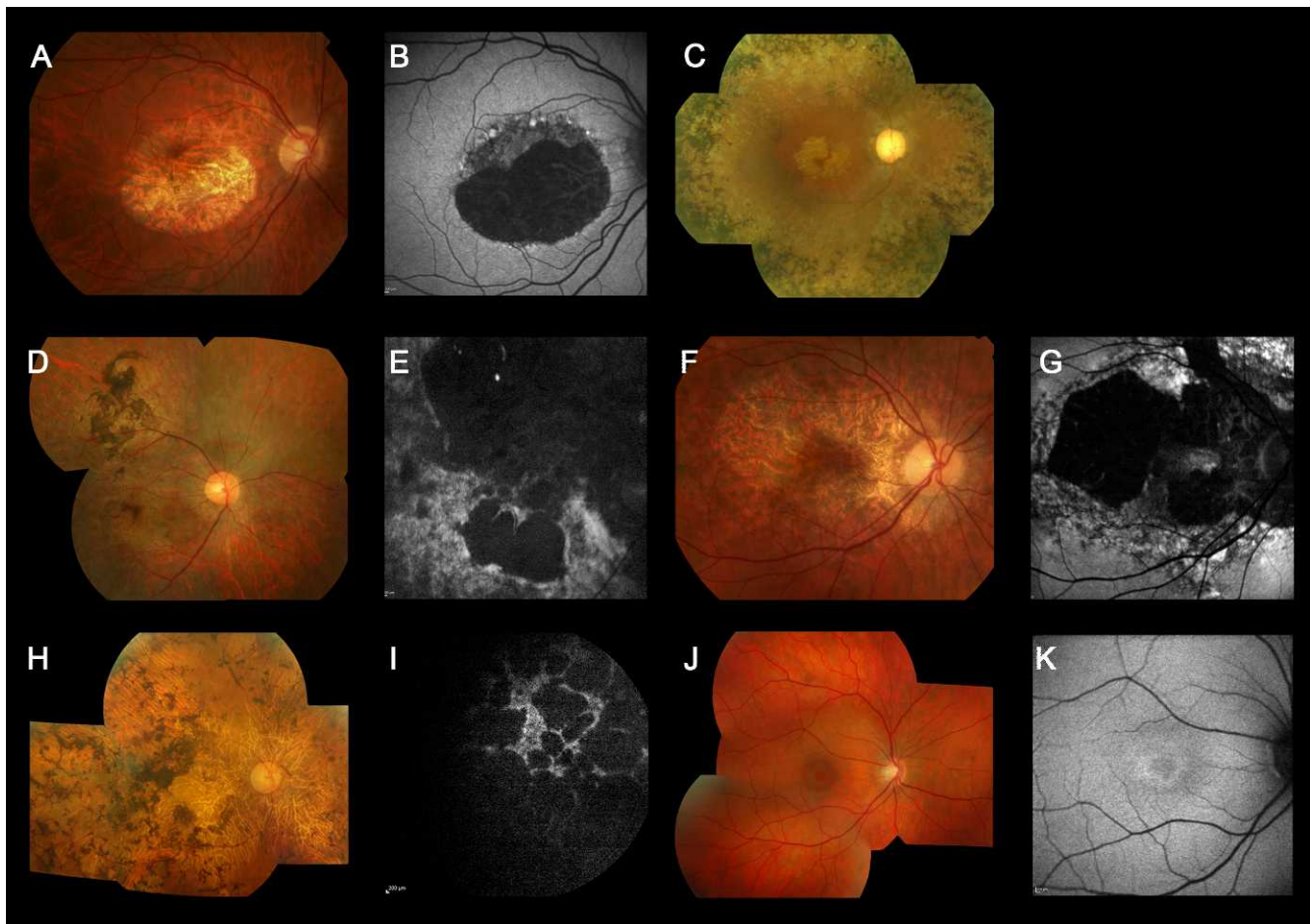


FIGURE 2. Color fundus photographs and autofluorescence images of six cases harboring a single, likely benign, missense variant with “atypical” clinical features for *ABCA4*-associated retinal disease (patients 74, 75, 76, 77, 78, and 79). Color photograph of patient 74 shows a geographic atrophy-like appearance (A), which on AF imaging is surrounded by foci of high and low AF signal (B). Patient 75 has evidence of generalized retinal atrophy in addition to marked macular atrophy, with dense pigmentation at the level of the RPE, and bone spicule formation, marked vessel attenuation, and optic disc pallor (C). Patient 76 has extensive macular atrophy extending beyond the arcades, with dense pigmentation at the level of the RPE and slight bone spicule pigmentation in the periphery (D). AF imaging demonstrates a heterogeneous background, but no peripapillary sparing (E). Patient 77 has a large area of macular atrophy extending to the optic disc (F), which on AF imaging is surrounded by an irregular low AF signal with foci of high and low signal, with no peripapillary sparing (G). Patient 78 has multiple widespread areas of atrophy with dense pigmentation at the level of RPE and bone spicule pigmentation in the periphery (H). AF imaging identifies multiple low signal areas with a heterogeneous background and no peripapillary sparing (I). Patient 79 has subtle atrophy confined to the fovea (J). AF imaging demonstrates a localized low AF signal at the fovea surrounded by a homogeneous background (K).

disease was calculated as the difference between age at onset and age at the latest examination.

Clinical Assessment

A full medical history was obtained and a comprehensive ophthalmologic examination was performed for all patients. Clinical assessment included best-corrected Snellen visual acuity (converted to equivalent logMAR visual acuity), fundus photography, autofluorescence (AF) imaging, spectral domain optical coherence tomography (SD-OCT), and electrophysiologic assessment.

Color fundus photography was performed with the TRC-50IA Retinal Fundus Camera (Topcon, Tokyo, Japan) and AF images were obtained using either an HRA 2 (excitation wavelength, 488 nm; barrier filter, 500 nm; field of view, 30 × 30°; Heidelberg Engineering, Heidelberg, Germany)³¹ or Spectralis with viewing module version 5.1.2.0 (excitation wavelength, 488 nm; barrier filter, 500 nm; fields of view, 30 × 30° and 55 × 55°; Heidelberg Engineering) after pupillary

dilation.³² Patients were classified into one of three AF subtypes based on a recent report in *ABCA4*-associated retinal disease³¹: type 1—localized low AF signal at the fovea surrounded by a homogeneous background, type 2—localized low AF signal at the macula surrounded by a heterogeneous background, and type 3—multiple areas of low AF signal at the posterior pole with a heterogeneous background. SD-OCT imaging was obtained with the Spectralis with viewing module version 5.1.2.0.³²

Electrophysiologic assessment included full-field electroretinography (ffERG) and pattern electroretinography (PERG) incorporating the standards of the International Society for Clinical Electrophysiology of Vision (ISCEV).^{33,34} All components of the ffERG and PERG were taken into account when classifying patients into one of the three electrophysiologic groups:^{4,35} group 1—patients with PERG P50 abnormality with normal ERGs, group 2—subjects with PERG P50 abnormality and additional generalized cone ERG abnormality (assessed with light adapted 30 Hz ERG and light adapted 3.0 ERG), and group 3—individuals with PERG P50 abnormality, and addi-

TABLE 2. Molecular Genetic Status Identified by NGS in 79 Patients With ABCA4-Related Retinal Disease

Pt	Allele 1 Detected by APEX			Allele 2 Detected by NGS			Allele 3 Detected by NGS			Total N of DC Variants	Comments
	DNA Change	Protein Change/Effect	Pred. Patho.	DNA Change	Protein Change/Effect	Pred. Patho.	DNA Change	Protein Change/Effect	Pred. Patho.		
1	c.161G>A	p.C54Y	DC	c.2297G>T	p.G766V	DC				2	
2	c.223T>G	p.C75G	DC	c.5088C>G	p.S1696R	DC				2	
3	c.740A>C	p.N247T	DC	c.1433T>C	p.I478T	B	c.2345G>A	p.W782*	DC	2	
4	c.768G>T	Splice site	DC							1	
5	c.1222C>T	p.R408*	DC	c.2568C>A	p.Y856*	DC				2	
6	c.1804C>T	p.R602W	DC	c.859-9T>C	Splice site	PDC				2	
7	c.1805G>A	p.R602Q	DC	c.5113C>T	p.R1705W	DC				2	
8	c.1922G>C	p.C641S	DC							1	
9	c.1957C>T	p.R653C	DC							1	
10	c.1957C>T	p.R653C	DC							1	
11	c.2588G>C	p.G863A	DC	c.655A>T	p.R219*	DC				2	Allele 2 (p.R219*) was APEX-false-negative
12	c.2588G>C	p.G863A	DC	c.1906C>T	p.Q636*	DC				2	
13	c.2588G>C	p.G863A	DC	c.1906C>T	p.Q636*	DC				2	
14	c.2588G>C	p.G863A	DC							1	
15	c.2588G>C	p.G863A	DC							1	
16	c.2894A>G	p.N965S	DC	c.3322C>T	p.R1108C	DC				2	Allele 2 (p.R1108C) was APEX-false-negative
17	c.3064G>A	p.E1022K	DC	c.6729+4_-+18delAGTTGGCCCTGGGGC	Splice site	DC				2	
18	c.3064G>A	p.E1022K	DC							1	
19	c.3208_3209insGT	p.S1071fs	DC	c.2942C>T	p.P981L	DC	c.6529G>A	p.D2177N	B	2	
20	c.3208_3209insGT	p.S1071fs	DC	c.1519G>T	p.D507Y	DC				2	
21	c.3208_3209insGT	p.S1071fs	DC	c.4634G>A	p.S1545N	DC				2	
22	c.3208_3209insGT	p.S1071fs	DC							1	
23	c.3292C>T	p.R1098C	DC	c.3299T>A	p.I1100N	DC				2	
24	c.3322C>T	p.R1108C	DC	c.4978delC	p.L1661*	DC				2	
25	c.3386G>A	p.R1129H	DC	c.3208_3209insGT	p.S1071fs	DC	c.4634G>A	p.S1545N	DC	3	Allele 2 (p.S1071fs) was APEX false-negative and allele 1 (p.R1129H) was NGS false-negative
26	c.4139C>T	p.P1380L	DC	c.3191-1G>T	Splice site	DC				2	
27	c.4139C>T	p.P1380L	DC	c.3398T>C	p.I1133T	PDC				2	
28	c.4139C>T	p.P1380L	DC	c.4070C>A	p.A1357E	DC				2	
29	c.4139C>T	p.P1380L	DC	c.4773G>C	Splice site	DC				2	
30	c.4139C>T	p.P1380L	DC							1	
31	c.4139C>T	p.P1380L	DC							1	
32	c.4139C>T	p.P1380L	DC							1	
33	c.4234C>T	p.Q1412*	DC							1	
34	c.4319T>C	p.F1440S	DC							1	
35	c.4328G>A	p.R1443H	DC	c.180delG	p.M61fs	DC				2	
36	c.4469G>A	p.C1490Y	DC	c.1726G>C	p.D576H	DC				2	
37	c.4469G>A	p.C1490Y	DC							1	
38	c.4537_4538insC	p.Q1513fs	DC	c.5578C>T	p.R1860W	DC				2	Allele 1 (p.Q1513fs) was NGS-false-negative
39	c.4577C>T	p.T1526M	DC							1	

TABLE 2. Continued

Pt	Allele 1 Detected by APEX			Allele 2 Detected by NGS			Allele 3 Detected by NGS			Total N of DC Variants	Comments
	DNA Change	Protein Change/ Effect	Pred. Patho.	DNA Change	Protein Change/ Effect	Pred. Patho.	DNA Change	Protein Change/ Effect	Pred. Patho.		
40	c.4926C>G	p.S1642R	DC	c.5041_5055del GTGGTTGCCCATCTGC	p.V1681_C1685del	DC			DC	2	
41	c.4956T>G	p.Y1652*	DC							1	
42	c.5018+2T>C	Splice site	DC							1	
43	c.5461-10T>C		DC	c.6385A>G	p.S2129G	PDC				2	
44	c.5461-10T>C		DC							1	
45	c.5461-10T>C		DC							1	
46	c.5461-10T>C		DC							1	
47	c.5461-10T>C		DC							1	
48	c.5461-10T>C		DC							1	
49	c.5461-10T>C		DC							1	
50	c.5461-10T>C		DC							1	
51	c.5585-1G>A	Splice site	DC							1	
52	c.5714+5G>A	Splice site	DC	c.6209C>G	p.T2070R	DC				2	
53	c.5882G>A	p.G1961E	DC	c.2686A>G	p.K896E	B				1	
54	c.5882G>A	p.G1961E	DC	c.3050+1G>C	Splice site	DC				2	
55	c.5882G>A	p.G1961E	DC	c.3392delC/3393C>G	p.A1131Gfs	DC				2	
56	c.5882G>A	p.G1961E	DC	c.4539+2T>G	Splice site	DC				2	
57	c.5882G>A	p.G1961E	DC	c.4552A>C	p.S1518R	DC				2	
58	c.5882G>A	p.G1961E	DC	c.5899-2delA	Splice site	DC				2	
59	c.5882G>A	p.G1961E	DC							1	
60	c.6079C>T	p.L2027F	DC	c.1906C>T	p.Q636*	DC				2	Allele 2 (p.R1108C) was APEX-false-negative
61	c.6079C>T	p.L2027F	DC	c.3322C>T	p.R1108C	DC				2	
62	c.6079C>T	p.L2027F	DC	c.3370G>T	p.D1124Y	DC				2	
63	c.6079C>T	p.L2027F	DC							1	
64	c.6089G>A	p.R2030Q	DC	c.4326C>A	p.N1442K	DC				2	
65	c.6445C>T	p.R2149*	DC							1	
66	c.6709A>C	p.T2237P	DC	c.5899-3_5899-2delTA	Splice site	DC				2	
67	c.2971G>C	p.G991R	B	c.4538A>G	p.Q1513R	DC				1	
68	c.3602T>G	p.L1201R	B	c.1749G>C	p.K583N	DC				1	
69	c.3602T>G	p.L1201R	B	c.1982_1983insG	p.A662fs	DC				1	
70	c.3602T>G	p.L1201R	B	c.2972G>T	p.G991V	DC				1	
71	c.4685T>C	p.I1562T	B	c.3289A>T	p.R1097*	DC				1	
72	c.6320G>A	p.R2107H	B	c.2510T>C	p.L837P	DC				1	
73	c.6320G>A	p.R2107H	B	c.4352+1G>A	Splice site	DC				1	
74	c.2701A>G	p.T901A	B							0	
75	c.3602T>G	p.L1201R	B							0	
76	c.4283C>T	p.T1428M	B							0	
77	c.466A>G	p.I156V	B							0	
78	c.466A>G	p.I156V	B							0	
79	c.4715C>T	p.T1572M	B							0	

Putative novel variants are shown in italics. Splice-site alteration (described as splice site) includes the change expected to affect splicing, for example, when the splice donor or splice acceptor site is changed, and the change that might affect splicing, for example, changes close to the splice donor or splice acceptor site, or in the first or last nucleotide of an exon. Two variants result in nucleotide substitution at the end of an exon and cause splice-site alteration (c.768G>T and c.4775G>C). B, benign; DC, disease-causing; PDC, possibly disease-causing; Pred. Patho, predicted pathogenicity; Pt, patient number.

TABLE 3. In Silico Analysis for Previously Reported Variants Identified in 79 Patients With ABCA4-Related Retinal Disease

Exon/ IVS	Nucleotide Substitution	Protein Change/ Effect	N of Alleles Identified	Pt	Method			Polyphen 2			HSF Matrix			Allele Freq. by EVS	Reference	Comment		
					APEX	NGS	Previous Report	SIFT	Tol. Index	Hum Var Score (0-1)	Pred.	Wt CV	Mt CV				Variation	CV %
3	c.161G>A	p.C54Y	1	1	✓	✓	Lewis RA, et al. ¹¹	Tol.	0.11	PRD	0.994	No change	1/13006	db SNP (rs150774447)				
3	c.223T>G	p.C75G	1	2	✓	✓	Lewis RA, et al. ¹¹	Del.	NA	POD	0.603	No change	ND					
5	c.466A>G	p.I156V	2	77, 78	✓	✓	Papatoianou M, et al. ¹⁶	Tol.	0.46	B	0.003	No change	16/13006	db SNP (rs112467008)	Benign			
6	c.655A>T	p.R219*	1	11	✓	✓	Xi Q, et al. ²⁷	Del.	NA	B	0.135	No change	ND					
6	c.740A>C	p.N247T	1	3	✓	✓	APEX	Del.	NA	B		No change	ND					
6	c.768G>T	Splice site	1	4	✓	✓	Klevering BJ, et al. ²²	Tol.	0.56	NA		Site broken (-17.51)	ND					
9	c.1222C>T	p.R408*	1	5	✓	✓	Webster AR, et al. ⁷	✓	✓	POD	0.688	Site broken (-42.54)	ND					
12	c.1726G>C	p.D576H	1	36	✓	✓	Downs K, et al. ²⁵	✓	✓	POD	0.688	Site broken (-42.54)	1/13006					
13	c.1804C>T	p.R602W	1	6	✓	✓	Lewis RA, et al. ¹¹	Del.	0.00	B	0.129	No change	ND	db SNP (rs 6179409)				
13	c.1805G>A	p.R602Q	1	7	✓	✓	Webster AR, et al. ⁷	Del.	0.04	PRD	0.513	New site (+59.14)	2/13006	db SNP (rs61749410)				
13	c.1906C>T	p.Q636*	3	12, 13, 60	✓	✓	Zernant J, et al. ⁵	✓	✓	PRD	0.008	No change	1/13006	db SNP (rs145961131)	Benign			
13	c.1922G>C	p.C641S	1	8	✓	✓	Steinri S, et al. ²⁴	Del.	0.00	PRD	0.981	No change	ND	db SNP (rs61749416)				
14	c.1957C>T	p.R653C	2	9, 10	✓	✓	Rivera A, et al. ¹⁷	Del.	0.00	PRD	0.999	No change	ND	db SNP (rs61749420)				
17	c.2588G>C	p.G863A/ p.DelG863	5	11, 12, 13, 14, 15	✓	✓	Lewis RA, et al. ¹¹ / Maugeri A, et al. ²⁹	Del.	0.00	PRD	0.996	No change	68/13006	db SNP (rs76157638)				
18	c.2701A>G	p.T901A	1	74	✓	✓	APEX	Tol.	0.82	B	0.008	No change	23/13006	db SNP (rs139655975)	Benign			
19	c.2894A>G	p.N965S	1	16	✓	✓	Lewis RA, et al. ¹¹	Del.	0.03	PRD	0.981	New site (+54.26)	ND	db SNP (rs201471607)				
20	c.2971G>C	p.G991R	1	67	✓	✓	Yatsenko AN, et al. ¹³	Del.	0.02	PRD	0.999	No change	28/13006	db SNP (rs147484266)	Benign			
22	c.3064G>A	p.E1022K	2	17, 18	✓	✓	Webster AR, et al. ⁷	Del.	0.00	PRD	1.000	No change	ND	db SNP (rs61749459)	False-negative in APEX in patient 25			
22	c.3208_3209insGT	p.S1071fs	5	19, 20, 21, 22, 25	✓	✓	APEX	Del.	0.00	PRD	0.999	No change	ND					
22	c.3292C>T	p.R1098C	1	23	✓	✓	Rivera A, et al. ¹⁷	Del.	NA	PRD	0.999	No change	ND					
22	c.3322C>T	p.R1108C	3	16, 24, 61	✓	✓	Rozet JM, et al. ¹⁰	Del.	0.00	PRD	0.986	No change	1/13006	db SNP (rs61750120)	False-negative in APEX in patients 16 and 61			
23	c.3386G>A	p.R1129H	1	25	✓	✓	Zernant J, et al. ⁵	Del.	0.00	PRD	0.989	No change	ND		False-negative in APEX in patients 16 and 61			
24	c.3602T>G	p.L1201R	4	72, 73, 74, 79	✓	✓	Lewis RA, et al. ¹¹	Tol.	0.37	B	0.052	New site (20.08)	416/13006	db SNP (rs61750126)	Benign			
28	c.4139C>T	p.P1380L	7	30, 31, 32, 33, 34, 35, 36	✓	✓	Lewis RA, et al. ¹¹	Del.	0.01	B	0.377	No change	2/13006	db SNP (rs61750130)				
28	c.4234C>T	p.Q1412*	1	33	✓	✓	Rivera A, et al. ¹⁷	Tol.	0.15	B	0.010	No change	ND	db SNP (rs61750137)	Benign			
29	c.4283C>T	p.T1428M	1	76	✓	✓	APEX	Del.	0.00	POD	0.744	No change	2/13006	db SNP (rs1800549)	Benign			
29	c.4319T>C	p.F1440S	1	34	✓	✓	Lewis RA, et al. ¹¹	Del.	0.00	POD	0.374	No change	ND	db SNP (rs61750141)				
29	c.4326C>A	p.N1442K	1	64	✓	✓	Zernant J, et al. ⁵	Tol.	NA	POD	0.999	No change	1/13006	db SNP (rs61750142)				
29	c.4328G>A	p.R1443H	1	35	✓	✓	Rivera A, et al. ¹⁷	Del.	0.02	PRD	0.999	WT site broken (-32.62)	ND					
IVS29	c.4352+1G>A	Splice site	1	73	✓	✓	Zernant J, et al. ⁵	Del.	0.00	PRD	0.994	No change	ND	db SNP (rs61751402)				
30	c.4469G>A	p.C1490Y	2	36, 37	✓	✓	Lewis RA, et al. ¹¹	Tol.	0.00	PRD	0.994	Site broken (-31.55)	ND					
30	c.4538A>G	p.Q1513R	1	67	✓	✓	Webster AR, et al. ⁷	Tol.	NA	Benign	0.043	No change	ND					

TABLE 3. Continued

Exon/ IVS	Nucleotide Substitution	Protein Change/ Effect	N of Alleles Identified	Pt	Method		SIFT		Polyphen 2		HSF Matrix			Allele Freq. by EVS	Reference	Comment
					APEX	NGS	Previous Report	Tol. Index	Hum Var Score (0–1)	Pred. (0–1)	Site	Wt CV	Mt CV			
30	c.457_458insC	p.G1513fs	1	38	✓	Briggs CE, et al. ¹⁹	Del.	0.00	PRD	0.910	PRD	No change	ND	db SNP (rs61750152)	False-negative in NGS in patient 38	
31	c.4577C>T	p.T1526M	1	39	✓	Lewis RA, et al. ¹¹	Tol.	NA	PRD	0.783	PRD	No change	ND	db SNP (rs61750641)	Benign	
33	c.4685T>C	p.I1562T	1	71	✓	Yatsenko, et al. ¹⁵	Del.	0.02	B	0.326	B	No change	ND	db SNP (rs185093512)	Benign	
33	c.4715C>T	p.T1572M	1	79	✓	Pang CP and Lamm DS ²³	Del.	0.68	B	0.116	B	No change	ND	db SNP (rs61750561)	Benign	
35	c.4926C>G	p.S1642R	1	40	✓	Birch DG, et al. ²²	Tol.	0.68	B	0.116	B	No change	ND	db SNP (rs61753017)	Benign	
35	c.4956T>G	p.Y1652*	1	41	✓	Fumagalli A, et al. ¹⁶	Del.	NA	PRD	0.996	PRD	No change	ND	db SNP (rs61750561)	Benign	
IVS35	c.5018+2T>C	Splice site	1	42	✓	APEX	Del.	NA	PRD	0.996	PRD	No change	ND	db SNP (rs1800728)	Benign	
36	c.5113C>T	p.R1705W	1	7	✓	Ernest PJ, et al. ²⁶	Del.	NA	PRD	0.996	PRD	No change	ND	db SNP (rs1800728)	Benign	
IVS38	c.5461+10T>C	Splice site	8	43, 44, 45, 46, 47, 48, 49, 50	✓	Briggs CE, et al. ¹⁹	Del.	NA	PRD	0.996	PRD	No change	ND	db SNP (rs1800728)	Benign	
IVS39	c.5585-1G>A	Splice site	1	51	✓	Shroyer NF, et al. ²¹	Del.	NA	PRD	0.996	PRD	No change	ND	db SNP (rs1800728)	Benign	
IVS40	c.5714+5G>A	Splice site	1	52	✓	Cremers FP, et al. ⁸	Del.	NA	PRD	0.996	PRD	No change	ND	db SNP (rs1800728)	Benign	
42	c.5882G>A	p.G1961E	7	53, 54, 55, 56, 57, 58, 59	✓	Lewis RA, et al. ¹¹	Del.	0.00	PRD	0.998	PRD	No change	ND	db SNP (rs1800553)	Benign	
44	c.6079C>T	p.L2027F	4	60, 61, 62, 63	✓	Lewis RA, et al. ¹¹	Del.	0.00	PRD	1.000	PRD	No change	ND	db SNP (rs61751408)	Benign	
44	c.6089G>A	p.R2030Q	1	64	✓	Lewis RA, et al. ¹¹	Del.	0.00	PRD	0.995	PRD	No change	ND	db SNP (rs61750641)	Benign	
46	c.6320G>A	p.R2107H	2	72, 73	✓	Fishman GA, et al. ¹⁵	Del.	0.04	PRD	0.999	PRD	No change	ND	db SNP (rs62642564)	Benign	
47	c.6445C>T	p.R2149*	1	65	✓	Lewis RA, et al. ¹⁴	Del.	0.41	B	0.004	B	No change	ND	db SNP (rs61750654)	Benign	
48	c.6529G>A	p.D2177N	1	19	✓	Rivera A, et al. ¹⁷	Tol.	0.41	B	0.004	B	No change	ND	db SNP (rs1800555)	Benign	
48	c.6709A>C	p.T2237P	1	66	✓	APEX	Del.	NA	POD	0.719	POD	No change	ND	db SNP (rs1800555)	Benign	
IVS48	c.6729+4_+18del	Splice site	1	17	✓	Littink KW, et al. ²⁸	Del.	NA	POD	0.719	POD	No change	ND	db SNP (rs1800555)	Benign	

AGTTGGCCCTGGGGC

Splice-site alteration (described as splice site) includes the change expected to affect splicing, for example, when the splice donor or splice acceptor site is changed, and the change that might affect splicing, for example, changes close to the splice donor or splice acceptor site, or in the first or last nucleotide of an exon. SIFT (version 4.0.4) results are reported to be tolerant if tolerance index is ≥ 0.05 or deleterious if tolerance index is < 0.05 . Polyphen-2 (version 2.1) appraises mutations qualitatively as benign, possibly damaging or probably damaging based on the model's false positive rate. The cDNA is numbered according to Ensemble transcript ID ENST00000370225, in which +1 is the A of the translation start codon. Human splicing finder version 2.4.1 was applied to predict the effect of each variant on splicing. The result from the HSF matrix indicates the values for the wild type (Wt) and mutant sequences. The larger the difference in values between the Wt and the mutant sequences suggests a greater chance that the variant can affect splicing. EVS denotes variants in the Exome Variant Server, NHLBI Exome Sequencing Project, Seattle, WA (accessed 01/04/2013; available in the public domain at <http://snp.gs.washington.edu/EVS>). Acc., Acceptor; Allele freq., allele frequency; CV, consensus values; Del., deleterious; Don., donor; EVS, exome variant server; HSF, human splicing finder; IVS, intervening sequence; Mt, mutant; NA, not available; ND, not detected; POD, possibly damaging; PRD, probably damaging; Pred., prediction; Tol., tolerant.

TABLE 4. Numbers and Types of Variants Detected by APEX Technology and NGS

	Null					Non-Null		
	Total	Splice-Site		Frameshift	Unknown	In-Frame Deletion	Disease-Causing Missense	Benign Missense
		Altering	Nonsense					
Variants detected by prescreening with APEX	42	4	4	2	1	0	23	8
New variants detected by NGS alone	42 (33)	9 (7)	6 (4)	3 (3)	0 (0)	1 (1)	20 (16)	3 (2)
Gross total	84 (33)	13 (7)	10 (4)	5 (3)	1 (0)	1 (1)	43 (16)	11 (2)

Numbers in parentheses indicate the numbers of novel variants that have never been reported. Two variants were detected only on APEX array, but not identified by NGS; one frameshift variant (p.Q1513fs) and one disease-causing missense variant (p.R1129H).

tional generalized cone and rod ERG abnormality (assessed using dark adapted 0.01 dim flash ERG and dark adapted 11.0 bright flash ERG).

Genetic Screening

Blood samples were collected in EDTA tubes and DNA was extracted with a Nucleon Genomic DNA extraction kit (BACC2; Tepnel Life Sciences, Manchester, UK). Mutation prescreening of *ABCA4* was performed with the APEX microarray (ABCR400 chip or ABCR600 chip; Asper Ophthalmics, Tartu, Estonia; available in the public domain at <http://www.asperbio.com/genetic-tests/panel-of-genetic-tests/stargardt-disease-cone-rod-dystrophy-abca4>) in all probands.¹⁴ We screened 17 patients with ABCR400 (432 mutations on the chip) in 2005, 32 with updated ABCR400 (456 mutations) in 2006, 3 with further updated ABCR400 (480 mutations) in 2007, and 27 with ABCR500 (552 mutations) in 2011.

All 50 *ABCA4* exons and exon-intron boundaries were amplified with tagged PCR primers using an amplicon tagging protocol (Access Array; Fluidigm, South San Francisco, CA; available in the public domain at <http://www.fluidigm.com/products/access-array.html>) and NGS on the Roche 454 platform (Roche Applied Science, Penzberg, Upper Bavaria, Germany) was performed as reported previously.⁵ Sequences of the barcoded samples were analyzed with the NextGENE software for next generation sequence analysis (SoftGenetics, State College, PA), which mapped reads to the reference genome (HG19) and identified all the differences compared to the reference sequence. All the identified variants were confirmed by Sanger sequencing. Segregation analysis was not performed in this study.

In Silico Molecular Genetic Analysis

All the missense variants identified were analyzed using two software prediction programs: Sorting Intolerant From Tolerant (SIFT; available in the public domain at <http://sift.jvci.org>),³⁶ and PolyPhen2 (available in the public domain at <http://genetics.bwh.harvard.edu/pph/index.html>).³⁷ Predicted effects on splicing of all the missense and intronic variants were assessed with the Human Splicing Finder (HSF) program version 2.4.1 (available in the public domain at <http://www.umd.be/HSF>). The allele frequency of all the variants was estimated by reference to the Exome Variant Server (EVS; NHLBI Exome Sequencing Project, Seattle, WA; available in the public domain at <http://snp.gs.washington.edu/EVS>).

All the variants identified were classified into one of three categories based on the bioinformatics prediction protocol described in a previous report,⁵ namely disease-causing, possibly disease-causing, and benign. For the purpose of analysis in this study, variants predicted to be possibly

disease-causing were included in the total number of variants described as disease-causing variants. The nomenclature of the variants was in the main in keeping with the internationally established guidelines (available in the public domain at <http://www.hgvs.org/mutnomen>).³⁸

RESULTS

Clinical Findings

The clinical findings of the cohort are summarized in Table 1. The study included 40 male (51%) and 39 female (49%) unrelated probands. The median age at onset was 22.0 years, with a median duration of disease of 10.0 years. The median age at the latest examination was 40.0 years, with the median logMAR visual acuities being 1.00. Color fundus photographs were obtained in 75 patients and AF imaging was undertaken in 71 subjects. There were 21 patients (30%) with a type 1 AF pattern, 34 (48%) with type 2, and 16 (22%) with type 3. Of the 70 patients with available electrophysiologic data, 34 subjects (49%) were in ERG group 1 (isolated macular dysfunction), 7 (10%) in ERG group 2 (macular and generalized cone dysfunction), and 29 (41%) in ERG group 3 (macular and generalized cone and rod dysfunction).

Color fundus photographs, AF images, and SD-OCT of three representative cases of "typical" *ABCA4*-associated retinal disease are shown in Figure 1 (patients 19, 36, and 17), all harboring two disease-causing variants. Six cases with an "atypical" phenotype for *ABCA4*-associated retinal disease are shown in Figure 2 (patients 74–79), all of them carried only one, likely benign, *ABCA4* variant (Table 2).

Prescreening With APEX Technology

The results of prescreening of *ABCA4* in our cohort of 79 patients are summarized in Table 2. We detected 42 variants at the APEX prescreening stage. In silico analysis of these 42 variants suggested that 34 were disease-causing and 8 were considered benign. Therefore, these analyses confirmed at least one disease-causing variant in 66/79 patients, while 13/79 subjects had no disease-causing variants (Tables 2, 3).

Identification of New Variants by NGS

The results of NGS screening in our cohort of 79 patients are summarized in Table 2. We identified 82 variants by NGS in total; 53 missense, 13 splice-site alterations, 10 nonsense, four frameshifts, one in-frame deletion, and one intronic variant of unknown effect (Tables 2, 4). Of a total of 84 different variants identified in this study by APEX and NGS, there were two "NGS false-negative" variants (p.R1129H and p.Q1513fs), which were detected on APEX array, but were not detected by NGS (Table 2, patients 25 and 38).

TABLE 5. In Silico Molecular Genetic Analysis for Novel ABCA4 Variants Identified by NGS

Exon/ IVS	DNA Change	Protein Change/ Effect	N of Alleles Identified	Pt	SIFT		Polyphen2		HSF Matrix						Reference	Comments
					Pred. (0-1)	Tol. Index (0-1)	Pred.	Hum Var Score (0-1)	Wt CV	Mt CV	CV % Variation	Allele Freq. by EVS				
3 IVS7	c.180delG	p.M61fs	1	35					Acc.	78.18	76.99	Possibly site broken	ND	Possibly disease- causing		
	c.8599T>C	Splice site	1	5									ND			
11	c.1433T>C	p.I478T	1	1	Tol.	B	0.007					No change	ND	Benign		
	c.1519G>T	p.D507Y	1	20	Del.	POD	0.641					No change	1/13006		dbSNP (rs148234178)	
12	c.1749G>C	p.K583N	1	68	Del.	POD	0.893		Acc.	66.17	37.22	Site broken	1/13006	dbSNP (rs145265791)		
14	c.1982_ 1983insG	p.A662fs	1	69									ND			
	c.2297G>T	p.G766V	1	1	Tol.	NA	0.557		Don.	69.18	42.34	Site broken	ND			
15	c.2345G>A	p.W782*	1	3									ND			
	c.2510T>C	p.L837P	1	72	Tol.	NA	0.905					No change	ND			
16	c.2568C>A	p.Y856*	1	5									ND			
	c.2686A>G	p.K896E	1	53	Tol.	NA	0.002						ND	Benign		
20	c.2942C>T	p.P981L	1	19	Del.	0.00	0.813					No change	1/13006		dbSNP (rs147826775)	
20	c.2972G>T	p.G991V	1	70	Del.	NA	0.998		Donor	64.62	91.45	New site	ND			
IVS20	c.3050+1G>C	Splice site	1	54					Acc.	86.43	57.49	Site broken	ND			
	c.3191-1G>T	Splice site	1	26					Acc.	94.38	65.44	WT site broken	ND			
22	c.3289A>T	p.R1097*	1	71									ND			
	c.3299T>A	p.I1100N	1	23	Del.	NA	0.986					No change	ND			
23	c.3370G>T	p.D1124Y	1	62	Del.	NA	0.998					No change	ND			
	c.3392delC/ 3393C>G	p.A1131Gfs	1	55									ND			
23	c.3398T>C	p.I1133T	1	27	Del.	NA	0.100					No change	ND	Possibly disease- causing		
27	c.4070C>A	p.A1357E	1	28	Del.	NA	0.94		Acc.	40.92	69.86	New site	ND			
IVS30	c.4539+2T>G	Splice site	1	56					Don.	79.18	52.35	WT site broken	ND			
31	c.4552A>C	p.S1518R	1	57	Del.	NA	0.871		Acc.	76.3	47.36	Site broken	ND			
	c.4634G>A	p.S1545N	2	21, 25	Tol.	NA	0.253		Acc.	80.04	51.1	Site broken	ND			

TABLE 5. Continued

Exon/ IVS	DNA Change	Protein Change/ Effect	N of Alleles Identified	SIFT		Polyphen2		HSF Matrix				Comments		
				Pt Pred.	Tol Index (0-1)	Hum Var Score (0-1)	Site	Wt CV	Mt CV	CV % Variation	Allele Freq. by EVS		Reference	
33	c.4773G>C	Splice site	1	29	Don.	84.58	73.57	Site broken (-13.02)	ND					
35	c.4978delC	p.L1661*	1	24					ND					
36	c.5041_5055del GTGGTTGCCATCTGC	p.V1681_C1685del	1	40				NA	ND		db SNP (rs62646872)			
36	c.5088C>G	p.S1696R	1	10	Tol.	NA	PRD	0.780	Don.	59.34	86.17	New site (45.23)	ND	
39	c.5578C>T	p.R1860W	1	38	Del.	0.02	B	0.025				No change	ND	db SNP (rs200849015)
IVS42	c.5899-3_5899-2delTA	Splice site	1	66								NA	ND	
IVS42	c.5899-24delA	Splice site	1	58					Acc.	82.1	28.26	WT site broken (-65.58)	ND	
45	c.6209C>G	p.T2070R	1	52	Tol.	NA	PRD	0.996	Acc.	57.41	86.36	New site (50.42)	ND	
46	c.6385A>G	p.S2129G	1	43	Del.	NA	B	0.001					ND	Possibly disease- causing

Splice-site alteration (described as splice site) includes the change expected to affect splicing, for example, when the splice donor or splice acceptor site is changed, and the change that might affect splicing, for example, changes close to the splice donor or splice acceptor site, or in the first or last nucleotide of an exon. SIFT (version 4.0.4) results are reported to be tolerant if tolerance index is ≥ 0.05 or deleterious if tolerance index is < 0.05 . Polyphen-2 (version 2.1) appraises mutations qualitatively as benign, possibly damaging or probably damaging based on the model's false positive rate. The cDNA is numbered according to Ensemble transcript ID ENST00000370225, in which +1 is the A of the translation start codon. Human splicing finder version 2.4.1 was applied to predict the effect of each variant on splicing. The result from the HSF matrix indicates the values for the Wt and mutant sequences. The larger the difference in values between the Wt and the mutant sequences suggests a greater chance that the variant can affect splicing. EVS denotes variants in the Exome Variant Server, NHLBI Exome Sequencing Project, Seattle, WA (accessed 01/04/2013; available in the public domain at <http://snp.gs.washington.edu/EVS>).

TABLE 6. Distribution of 79 Patients With ABCA4-Related Retinal Disease Based on Number of Identified Disease-Causing Variants

		Comprehensive Screening With APEX and NGS			
		No Disease-Causing Variant	1 Disease-Causing Variant	2 Disease-Causing Variants	3 Disease-Causing Variants
Prescreening	1 disease causing-variant, <i>n</i> = 66		29	36	1
with APEX	No disease-causing variants, <i>n</i> = 13	6	7		
	Total, <i>n</i> = 79	6	36	36	1

A total of 42 additional variants, which were not detected by APEX, were identified in 45 (57%) patients screened by NGS (Tables 2, 4). Three variants (p.R219*, p.R1108C, and p.S1071fs) found by NGS, were not identified by APEX at the prescreening stage despite being represented on the array ("APEX false-negative"; Table 2, patients 11, 16, 25, and 61). Three (3/45) subjects had two new variants and 42 (42/45) individuals had one new variant (Table 2). Of the 42 new variants detected by NGS, there were 23 missense, 9 splice-site alterations, 6 nonsense, 3 frameshifts, and 1 in-frame deletion (Table 4).

Of the 42 new variants identified by NGS, 33 (79%) were novel, including 18 missense, 7 splice-site alterations, 4 nonsense, 3 frameshifts, and 1 in-frame deletion (Tables 2, 4, 5). Seven variants identified only by NGS already were known, but not yet added to the ABCA4 array by the time of the prescreening of those samples.

In Silico Molecular Genetic Analysis for New Variants Identified by NGS

In silico analysis of the 42 variants identified by NGS, including the 9 previously reported variants and the 33 novel variants, are shown in Tables 3 and 5, respectively.

Of the 9 previously reported variants that were detected by NGS, there were 4 null variants (2 nonsense and 2 splice-site alterations); 4 disease-causing missense variants, with deleterious or damaged protein function predicted by SIFT and Polyphen2; and one benign missense variant (p.D2177N, Table 3).

Deleterious or damaged protein function was predicted by SIFT and Polyphen2 in 16 of 18 novel missense variants (Table 5). Two variants (p.I478T and p.K896E) were predicted to be tolerated and benign. The predicted effects on splicing of these 16 missense variants, one variant resulting in a nucleotide substitution at the end of exon 33 (c.4773G>C), and five intronic variants, were assessed using the HSF program. Altered splicing was suggested for 7 of the missense variants, the (c.4773G>C) variant, and all 5 intronic variants (Table 5). The allele frequencies for the 33 novel variants were, at most, 1 in 13006, suggesting that these are all very rare. Overall, 31 of the 33 novel variants were considered disease-causing, except for only the two missense variants, p.I478T and p.K896E (Table 5).

Disease-Causing Variants

A total of 73 (31 novel and 42 previously identified) disease-causing variants was identified in this cohort of 79 patients (Table 4). The distribution of the number of alleles in the cohort is summarized in Table 6. One patient (1%) harbored three disease-causing variants, 36 (46%) had two disease-causing variants, 36 (46%) had one disease-causing variant, and six patients (7%) remained with no disease-causing variant identified (Table 6).

DISCUSSION

Our study reports the molecular genetic findings using a PCR-enrichment-based NGS strategy in a large well-characterized British cohort with a clinical diagnosis of ABCA4-associated retinal disease. The NGS revealed two or more disease-causing variants in 37 (47%) of 79 patients, in whom only one variant was detected in prescreening with APEX array technology.

Of the 66 subjects with one disease-causing allele identified previously by APEX, the second disease-causing allele was identified in 37 individuals (56%). In keeping with our findings, Zernant et al. reported that the same NGS strategy identified the second disease-causing allele in 48% of their cohort who also only had one allele found previously with APEX.⁵ These findings suggest that many disease-associated mutations in the ABCA4 gene are very rare and yet unknown, supporting the validity of the PCR-enrichment-based NGS method either as the screening method of choice, or as an additional screening method for patients in whom APEX does not reveal two variants. Of note, the NGS method is cost- and time-efficient at this time only for large (at least 96 samples) cohorts.

Of the 13 patients with initially no disease-causing variant found by APEX, one disease-causing ABCA4 allele was identified in seven subjects (54%) by NGS, with six remaining with no likely disease-causing allele (46%). Further screening with NGS, including screening all intronic regions, and upstream and downstream control regions of the ABCA4 gene, as well as other candidate genes, in larger well-characterized cohorts will be needed to identify fully all pathogenic alleles in these patients. It recently has been proposed that intronic and synonymous variants may account for a significant proportion of the remaining disease-causing variants not identified with exomic NGS.^{5,39}

There were two "NGS false negative" variants (p.R1129H and p.Q1513fs) and three "APEX false negative" variants (p.R219*, p.R1108C, and p.S1071fs) in our cohort. The missense variant p.R1129H was not detected by NGS, most likely due to allele-specific amplification. The frameshift variant c.4537_4538insC, p.Q1513fs, is located in a homopolymer of seven C-nucleotides, where an insertion of another C nucleotide presents a challenge to identify by the Roche 454 sequencing platform. The "APEX false negative" variants were caused by technical issues with the specific array, ABCR400 (432 mutations on the chip) in 2005. Two of those variants, p.R1108C, and p.S1071fs, were detected by APEX in other patients (Table 2). Nevertheless, these findings suggest that combined APEX/NGS analysis may be worthy of consideration for comprehensive mutation detection.

In silico molecular genetic analysis was performed for all 84 variants identified in our cohort, with 73 of these determined to be likely disease-causing. Review of the clinical findings of the six patients harboring only one, likely benign, missense variant, revealed that they had a less typical ("atypical") phenotype for ABCA4-associated retinal disease, including an absence of flecks in all patients, significant peripheral retinal bone spicule pigmentation in three subjects, geographic-like atrophy in one individual, a subtle atrophic change confined to

the fovea in one patient, and a lack of peripapillary sparing on AF imaging in three subjects. In this study, patients with bilateral macular atrophy, with or without surrounding flecks, potentially were included as having Stargardt disease, with other less typical (“atypical”) findings also having been reported in *ABCA4*-associated retinal disease.^{18,40,41} However, other genes associated with autosomal recessive macular dystrophy, autosomal recessive cone-rod dystrophy, and autosomal recessive retinitis pigmentosa also should be considered for these patients with no identified likely disease-causing *ABCA4* alleles, in addition to the possibility of missed *ABCA4* alleles due to the inherent limitations of the molecular testing approach.

In our cohort, in keeping with previous reports, there was one well-known intronic variant (c.5461-10T>C) of equivocal pathogenicity following detailed in silico analysis,^{4,5,16} highlighting the need for an effective assay to determine functionally the effects of *ABCA4* variants, or alternatively to consider investigating mRNA expression. The allele, c.5461-10T>C, was the most common in our cohort, with 8/79 patients (10%) harboring this variant. Interestingly, the second allele was not identified in six of these patients. However, cosegregation of c.5461-10T>C with the disease has been documented in several studies, thereby strongly suggesting its disease-causation.⁴

In summary, we have demonstrated the validity and utility of *ABCA4* mutation screening with an NGS-based protocol in a large British cohort, with successful identification of the new disease-causing alleles in approximately half of the cases harboring one allele detected by prescreening with APEX technology. The identification of both disease-causing alleles will improve the accuracy of diagnosis and the counselling of patients, and also will assist in more effective patient selection of genetically confirmed participants for current and future clinical trials for *ABCA4*-associated retinal disease.

Acknowledgments

The authors thank the patients who kindly agreed to take part in this study and colleagues who referred individuals to us at Moorfields Eye Hospital, and those who contributed to the assembly of the *ABCA4* panel, particularly Naushin Waseem, Bev Scott, and Sophie Devery. The authors also thank Graham E. Holder, Anthony G. Robson, and Magella M. Neveu for interpretation of electrophysiologic data, and Yozo Miyake, Arundhati Dev Borman, Rajarshi Mukherjee, Eva Lenassi, Panagiotis I. Sergouniotis, and Aman Chandra for their insightful comments.

Supported by grants from the National Institute for Health Research Biomedical Research Centre at Moorfields Eye Hospital NHS Foundation Trust and UCL Institute of Ophthalmology; Foundation Fighting Blindness (USA); Fight For Sight; Moorfields Eye Hospital Special Trustees; Macular Disease Society; National Eye Institute/NIH Grants EY021163, EY019861, and EY019007 (Core Support for Vision Research); unrestricted funds from Research to Prevent Blindness (New York, NY) to the Department of Ophthalmology; Columbia University; Suzuken Memorial Foundation; Mitsukoshi Health and Welfare Foundation; Daiwa Anglo-Japanese Foundation; and Grant-in-Aid for Young Scientists (B) of the Ministry of Education, Culture, Sports, Science, and Technology (Japan); and by a Foundation Fighting Blindness Career Development Award (MM). The authors alone are responsible for the content and writing of the paper.

Disclosure: **K. Fujinami**, None; **J. Zernant**, None; **R.K. Chana**, None; **G.A. Wright**, None; **K. Tsunoda**, None; **Y. Ozawa**, None; **K. Tsubota**, None; **A.R. Webster**, None; **A.T. Moore**, None; **R. Allikmets**, None; **M. Michaelides**, None

References

- Allikmets R, Singh N, Sun H, et al. A photoreceptor cell-specific ATP-binding transporter gene (ABCR) is mutated in recessive Stargardt macular dystrophy. *Nat Genet.* 1997;15:236-246.
- Michaelides M, Chen LL, Brantley MA Jr, et al. *ABCA4* mutations and discordant *ABCA4* alleles in patients and siblings with bull's-eye maculopathy. *Br J Ophthalmol.* 2007;91:1650-1655.
- Burke TR, Tsang SH. Allelic and phenotypic heterogeneity in *ABCA4* mutations. *Ophthalmic Genet.* 2011;32:165-174.
- Fujinami K, Lois N, Davidson AE, et al. A longitudinal study of Stargardt disease: clinical and electrophysiological assessment, progression and genotype correlations. *Am J Ophthalmol.* 2013;155:1075-1088.
- Zernant J, Schubert C, Im KM, et al. Analysis of the *ABCA4* gene by next-generation sequencing. *Invest Ophthalmol Vis Sci.* 2011;52:8479-8487.
- Fujinami K, Akahori M, Fukui M, Tsunoda K, Iwata T, Miyake Y. Stargardt disease with preserved central vision: identification of a putative novel mutation in ATP-binding cassette transporter gene. *Acta Ophthalmol.* 2011;89:297-298.
- Webster AR, Heon E, Lotery AJ, et al. An analysis of allelic variation in the *ABCA4* gene. *Invest Ophthalmol Vis Sci.* 2001;42:1179-1189.
- Cremers FP, van de Pol DJ, van Driel M, et al. Autosomal recessive retinitis pigmentosa and cone-rod dystrophy caused by splice site mutations in the Stargardt's disease gene ABCR. *Hum Mol Genet.* 1998;7:355-362.
- Martinez-Mir A, Paloma E, Allikmets R, et al. Retinitis pigmentosa caused by a homozygous mutation in the Stargardt disease gene ABCR. *Nat Genet.* 1998;18:11-12.
- Rozet JM, Gerber S, Souied E, et al. Spectrum of ABCR gene mutations in autosomal recessive macular dystrophies. *Eur J Hum Genet.* 1998;6:291-295.
- Lewis RA, Shroyer NF, Singh N, et al. Genotype/phenotype analysis of a photoreceptor-specific ATP-binding cassette transporter gene, ABCR, in Stargardt disease. *Am J Hum Genet.* 1999;64:422-434.
- Rozet JM, Gerber S, Ghazi I, et al. Mutations of the retinal specific ATP binding transporter gene (ABCR) in a single family segregating both autosomal recessive retinitis pigmentosa RP19 and Stargardt disease: evidence of clinical heterogeneity at this locus. *J Med Genet.* 1999;36:447-451.
- Yatsenko AN, Shroyer NF, Lewis RA, Lupski JR. Late-onset Stargardt disease is associated with missense mutations that map outside known functional regions of ABCR (*ABCA4*). *Hum Genet.* 2001;108:346-355.
- Jaakson K, Zernant J, Kulm M, et al. Genotyping microarray (gene chip) for the ABCR (*ABCA4*) gene. *Hum Mutat.* 2003;22:395-403.
- Fishman GA, Stone EM, Grover S, Derlacki DJ, Haines HL, Hockey RR. Variation of clinical expression in patients with Stargardt dystrophy and sequence variations in the ABCR gene. *Arch Ophthalmol.* 1999;117:504-510.
- Papaioannou M, Ocaka L, Bessant D, et al. An analysis of ABCR mutations in British patients with recessive retinal dystrophies. *Invest Ophthalmol Vis Sci.* 2000;41:16-19.
- Rivera A, White K, Stohr H, et al. A comprehensive survey of sequence variation in the *ABCA4* (ABCR) gene in Stargardt disease and age-related macular degeneration. *Am J Hum Genet.* 2000;67:800-813.
- Birch DG, Peters AY, Locke KL, Spencer R, Megarity CF, Travis GH. Visual function in patients with cone-rod dystrophy (CRD) associated with mutations in the *ABCA4*(ABCR) gene. *Exp Eye Res.* 2001;73:877-886.
- Briggs CE, Rucinski D, Rosenfeld PJ, Hirose T, Berson EL, Dryja TP. Mutations in ABCR (*ABCA4*) in patients with Stargardt

- macular degeneration or cone-rod degeneration. *Invest Ophthalmol Vis Sci.* 2001;42:2229-2236.
20. Fumagalli A, Ferrari M, Soriani N, et al. Mutational scanning of the ABCR gene with double-gradient denaturing-gradient gel electrophoresis (DG-DGGE) in Italian Stargardt disease patients. *Hum Genet.* 2001;109:326-338.
 21. Shroyer NF, Lewis RA, Yatsenko AN, Wensel TG, Lupski JR. cosegregation and functional analysis of mutant ABCR (ABCA4) alleles in families that manifest both Stargardt disease and age-related macular degeneration. *Hum Mol Genet.* 2001; 10:2671-2678.
 22. Klevering BJ, Blankenagel A, Maugeri A, Cremers FP, Hoyng CB, Rohrschneider K. Phenotypic spectrum of autosomal recessive cone-rod dystrophies caused by mutations in the ABCA4 (ABCR) gene. *Invest Ophthalmol Vis Sci.* 2002;43: 1980-1985.
 23. Pang CP, Lam DS. Differential occurrence of mutations causative of eye diseases in the Chinese population. *Hum Mutat.* 2002;19:189-208.
 24. Stenirri S, Fermo I, Battistella S, et al. Denaturing HPLC profiling of the ABCA4 gene for reliable detection of allelic variations. *Clin Chem.* 2004;50:1336-1343.
 25. Downs K, Zacks DN, Caruso R, et al. Molecular testing for hereditary retinal disease as part of clinical care. *Arch Ophthalmol.* 2007;125:252-258.
 26. Ernest PJ, Boon CJ, Klevering BJ, Hoefsloot LH, Hoyng CB. Outcome of ABCA4 microarray screening in routine clinical practice. *Mol Vis.* 2009;15:2841-2847.
 27. Xi Q, Li L, Traboulsi EI, Wang QK. Novel ABCA4 compound heterozygous mutations cause severe progressive autosomal recessive cone-rod dystrophy presenting as Stargardt disease. *Mol Vis.* 2009;15:638-645.
 28. Littink KW, Koenekoop RK, van den Born LI, et al. Homozygosity mapping in patients with cone-rod dystrophy: novel mutations and clinical characterizations. *Invest Ophthalmol Vis Sci.* 2010;51:5943-5951.
 29. Maugeri A, van Driel MA, van de Pol DJ, et al. The 2588G->C mutation in the ABCR gene is a mild frequent founder mutation in the Western European population and allows the classification of ABCR mutations in patients with Stargardt disease. *Am J Hum Genet.* 1999;64:1024-1035.
 30. Klevering BJ, Yzer S, Rohrschneider K, et al. Microarray-based mutation analysis of the ABCA4 (ABCR) gene in autosomal recessive cone-rod dystrophy and retinitis pigmentosa. *Eur J Hum Genet.* 2004;12:1024-1032.
 31. Fujinami K, Sergouniotis PI, Davidson AE, et al. The clinical effect of homozygous ABCA4 alleles in 18 patients [published online ahead of print June 11, 2013]. *Ophthalmology.* doi:10.1016/j.ophtha.2013.04.016.
 32. Sergouniotis PI, Davidson AE, Lenassi E, Devery SR, Moore AT, Webster AR. Retinal structure, function, and molecular pathologic features in gyrate atrophy. *Ophthalmology.* 2012; 119:596-605.
 33. Bach M, Brigell MG, Hawlina M, et al. ISCEV standard for clinical pattern electroretinography (PERG): 2012 update. *Doc Ophthalmol.* 2013;126:1-7.
 34. Marmor MF, Fulton AB, Holder GE, Miyake Y, Brigell M, Bach M. ISCEV standard for full-field clinical electroretinography (2008 update). *Doc Ophthalmol.* 2009;118:69-77.
 35. Lois N, Holder GE, Bunce C, Fitzke FW, Bird AC. Phenotypic subtypes of Stargardt macular dystrophy-fundus flavimaculatus. *Arch Ophthalmol.* 2001;119:359-369.
 36. Ng PC, Henikoff S. SIFT: predicting amino acid changes that affect protein function. *Nucleic Acids Res.* 2003;31:3812-3814.
 37. Adzhubei IA, Schmidt S, Peshkin L, et al. A method and server for predicting damaging missense mutations. *Nat Methods.* 2010;7:248-249.
 38. den Dunnen JT, Antonarakis SE. Mutation nomenclature extensions and suggestions to describe complex mutations: a discussion. *Hum Mut.* 2000;15:7-12.
 39. Braun TA, Mullins RF, Wagner AH, et al. Non-exonic and synonymous variants in ABCA4 are an important cause of Stargardt disease. *Hum Mol Genet.* In press.
 40. Burke TR, Allikmets R, Smith RT, Gouras P, Tsang SH. Loss of peripapillary sparing in non-group I Stargardt disease. *Exp Eye Res.* 2010;91:592-600.
 41. Fritsche LG, Fleckenstein M, Fiebig BS, et al. A subgroup of age-related macular degeneration is associated with mono-allelic sequence variants in the ABCA4 gene. *Invest Ophthalmol Vis Sci.* 2012;53:2112-2118.